4. A Review of the Microstructural Aspects of Cleavage Fracture

JOHN R. LOW, JR.

General Electric Research Laboratory
Schenectady, New York

ABSTRACT

Deductions drawn from observations of fracture surfaces concerning the influence of microstructure on cleavage fracture are here reviewed. The observations on single crystals are first discussed, followed by a discussion of polycrystalline single-phase aggregates and the effects introduced by grain boundaries. As an example of a two-phase aggregate, the observations made on the cleavage fracture of steel in the pearlitic, bainitic, and martensitic conditions are described, and reasons for the superior properties of lower bainite and martensite are suggested. Finally, a number of cases of intergranular brittle fracture are discussed, and the importance of distinguishing between transcrystalline and intercrystalline fracture is pointed out.

Cleavage Fracture of Single Crystals

In an ideally perfect crystal parted by cleavage, one would expect the two surfaces created by the cleavage to be perfectly plane and to exhibit no structure. Cleavage surfaces approaching this degree of perfection have sometimes been observed. For example, by rapidly cleaving carefully grown zinc crystals at 78°K, surfaces can be achieved on which it is impossible to focus with the light microscope. Tolansky also reports that mica cleavages may be perfect to within 30 Å over distances of the order of a millimeter.[1]

It is usual, however, to observe so-called "river patterns," such as the one illustrated in Fig. 1, if the cleavage surface is examined microscopically. Each of the lines making up the river pattern of Fig. 1 represents

a level difference in the cleavage surface resulting from the fact that the cleavage crack, instead of following a single crystallographic plane, has been broken up by defects in the crystal structure. A crack that originally may have been ideally plane becomes, after some growth, a whole set of parallel cracks propagating simultaneously and joining along lines where they overlap, either by secondary cleavage or by shearing off

Fig. 1. Cleavage step "river pattern." 3% Si-Fe single-crystal cleavage surface. Cleaved at 78°K. Direction of crack propagation is from top to bottom of the photograph. Note low-angle tilt boundary.

of a thin strip of the crystal. This latter process is illustrated schematically in Fig. 2. Other processes have been suggested by Gilman [2] and Berry.[3] The importance of these cleavage steps arises from the fact that, for a cleavage step to form, additional energy is required, and the propagation of the cleavage crack is therefore made more difficult.[4] Thus, in addition to the surface energy and kinetic energy which must be supplied to propagate the crack,[5] an additional amount of energy, some of which has been absorbed in the formation of cleavage steps, must be supplied by the available elastic strain energy if the crack is to continue to propa-

gate. The amount of energy absorbed in cleavage step formation for some typical cases has been estimated by Gilman.[2]

Cleavage steps may arise from a number of causes;[4] by far the most common is the presence of screw dislocations that cut the cleavage plane.[6,7]

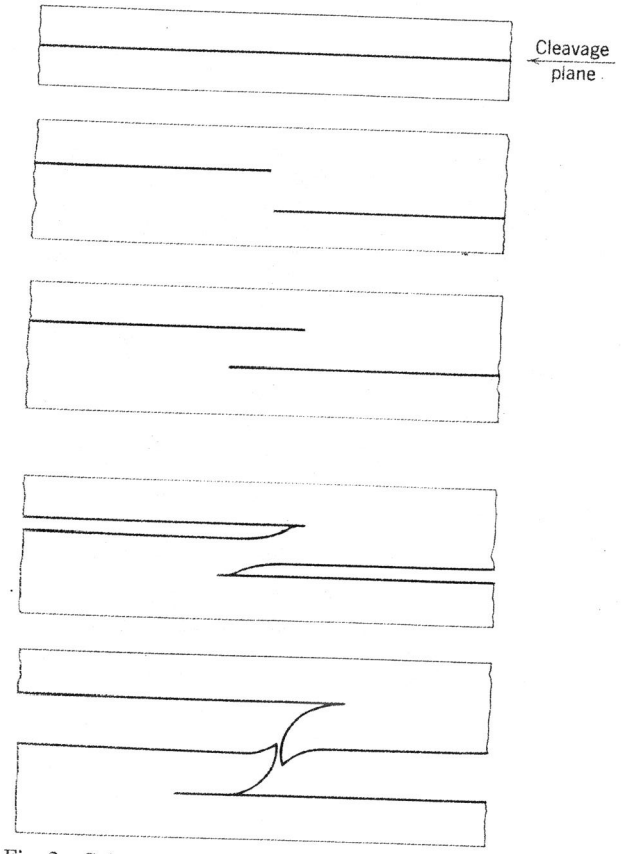

Fig. 2. Schematic representation of cleavage step formation between two parallel cleavage cracks on differing crystal planes. Ductile fracture shown is one mode of parting to form steps; for others, see Gilman[2] and Berry.[3]

As a cleavage crack front passes a screw dislocation, the levels of the crack on either side of the dislocation are shifted with respect to each other. After the crack front has passed the dislocation, it moves on two different levels which are joined by a unit cleavage step of the order of one Burgers vector in height. Such cleavage steps will tend to run together,[4] either canceling each other if they are of opposite sign or producing a larger

cleavage step if they are of the same sign. Both of these processes may be seen in the cleavage step pattern of Fig. 1.

The screw dislocations responsible for cleavage steps may be introduced into the crystal in several ways. They may be part of the network of randomly distributed, grown-in dislocations present in any real crystal. They may be present as regular arrays, as in a low-angle twist boundary.[4,7] Finally, they may be introduced by plastic deformation, either by deformation of the whole crystal before cleavage occurs,[8,9] or by glide at the tip of the cleavage crack. The latter case arises only if the crack velocity is low enough or if the temperature at which this cleavage occurs is high enough.[4,8,9]

Examples of the sudden increase in the number of cleavage steps that occur when a crack crosses a low-angle twist boundary are shown in Figs. 3 and, 4. The effect of these cleavage steps is to reduce the crack, velocity, and, if only a portion of the crack front crosses the twist boundary, then this portion of the crack front lags behind the balance. As might be expected, edge dislocations do not produce cleavage steps,[8] and arrays of dislocations in small-angle tilt boundaries simply produce a change in direction of crack propagation without increasing the energy required for propagation. This difference between tilt and twist boundaries may be observed by comparing Fig. 1 (tilt boundary) and Fig. 3 (twist boundary). The cleavage step pattern in Fig. 1 is unaffected by the tilt boundary.

Screw dislocations capable of producing cleavage steps may be introduced into a crystal by glide at the tip of a cleavage crack. The requirements for glide to occur at the tip of a moving crack have been analyzed by Gilman.[9] The essential condition is that the crack velocity must be low enough so that the time of loading of a unit volume at the tip of the moving crack is long enough for dislocations to move and multiply. Since the velocity of motion of a dislocation is a function of both the stress and the temperature,[10] a decrease in the velocity of the crack front or an increase in the temperature will permit glide to occur in advance of the crack; cleavage steps will result. Figure 5 illustrates the glide that occurs when a high-velocity crack in LiF is allowed to slow down and stop.[11] The effect of this glide on the cleavage process is illustrated for a silicon-iron crystal in Fig. 6 and for a LiF crystal in Fig. 7. Figure 7 shows that there is a one-to-one correspondence between the etch pit pattern delineating the regions of crack-nucleated glide and the cleavage step pattern on the matching, unetched cleavage surface.

By varying the velocity of cleavage crack propagation in LiF and then etch pitting the cleavage surfaces produced at different crack velocities, Gilman[9] finds a critical crack velocity V^* above which dislocations are not nucleated by the stresses at the tip of the moving crack. This critical

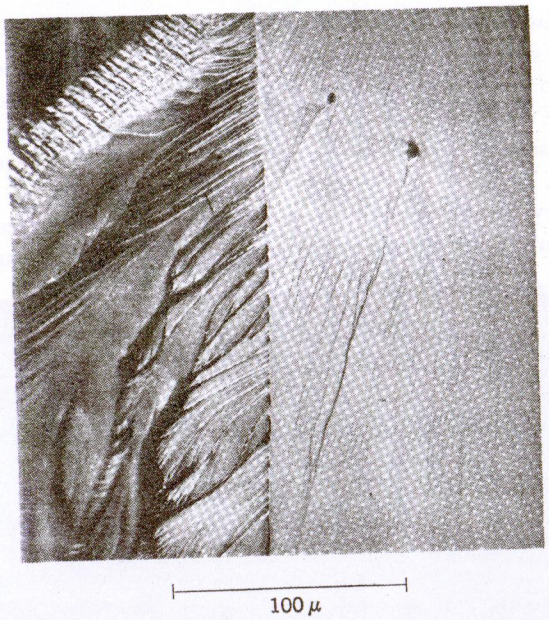

Fig. 3. Increase in cleavage step density for crack crossing 3° twist boundary in 3% Si-Fe crystal cleaved at 78°K. Direction of crack propagation was from upper right to lower left.

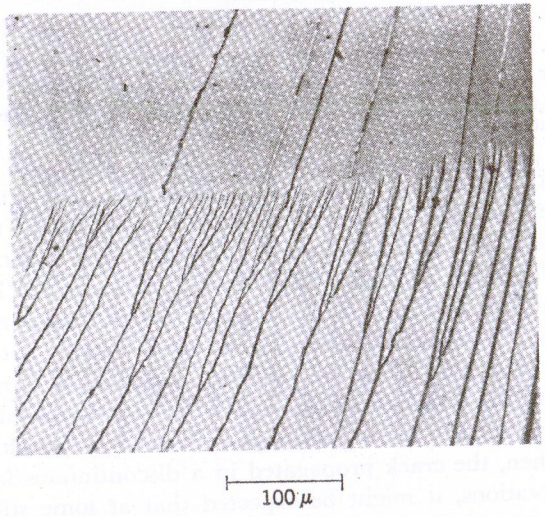

Fig. 4. Creation of cleavage steps at tilt-twist boundary in LiF. Crack moved from top to bottom. Boundary: approximately 0.85° twist, 0.87° tilt. (Courtesy J. J. Gilman.[7])

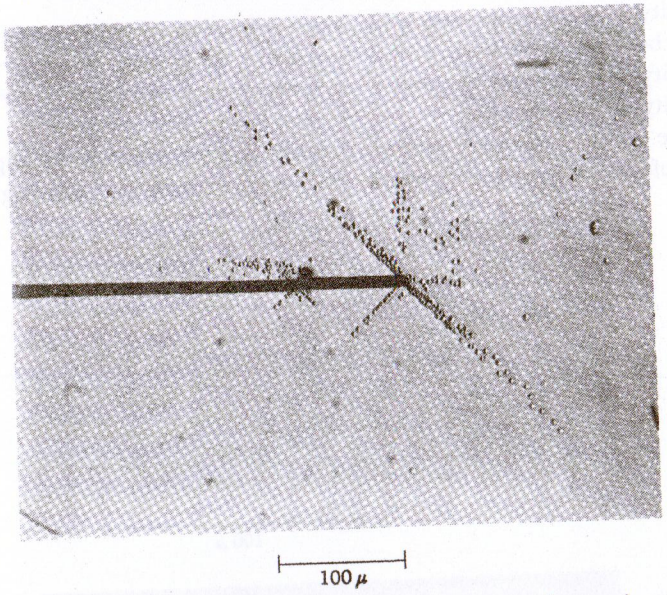

Fig. 5. Etch-pit pattern showing dislocations nucleated at tip of stopped crack in LiF. Crack tip rounded and crack widened by polishing and etching procedures. (Courtesy J. J. Gilman.[9])

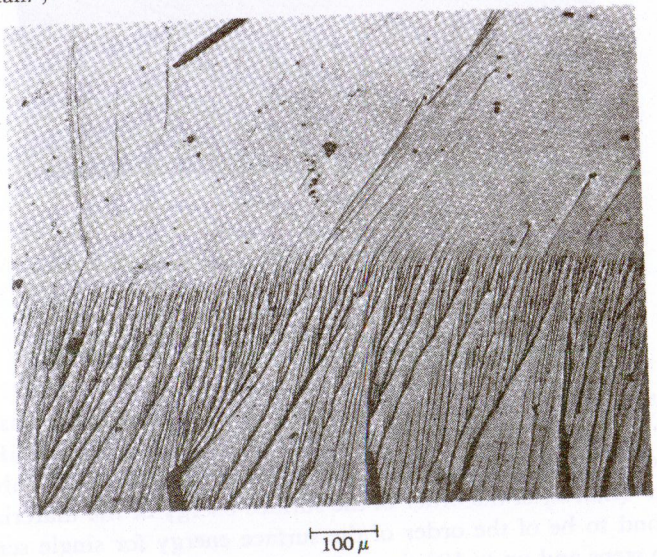

Fig. 6. Cleavage steps originating at point where cleavage crack was stopped and restarted immediately at 78°K in 3% Si-Fe crystal. Direction of propagation upper right to lower left.

velocity at room temperature was found to be about 6×10^3 cm/sec, which may be compared with a value of 2.0×10^5 cm/sec for the terminal velocity of crack propagation [2] and with a value of 6.5×10^5 for the velocity of sound in LiF.

The effect of glide at the tip of a crack at low velocities of propagation is twofold: Energy is absorbed in the nucleation and propagation of

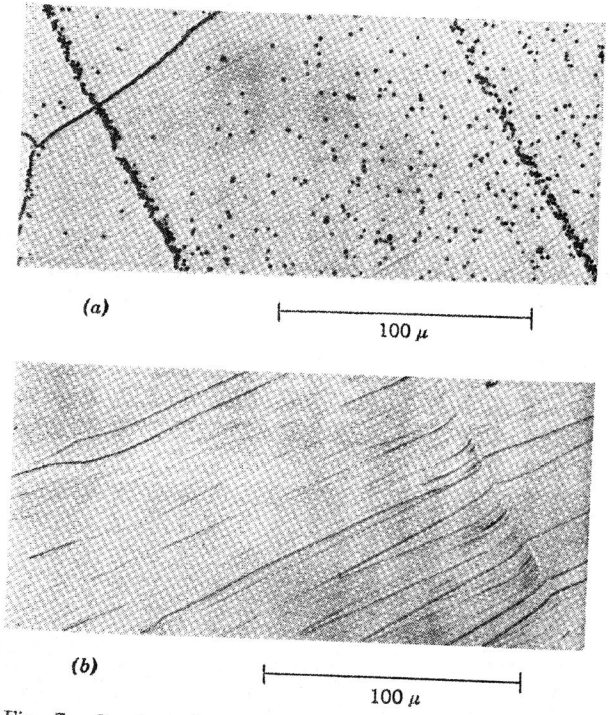

Fig. 7. Crack-nucleated dislocations and associated cleavage steps in LiF. Crack moved from upper right to lower left. (*a*) One cleavage surface of cracked crystal etch-pitted to reveal dislocations. (*b*) Matching cleavage surface, as cleaved. (Courtesy J. J. Gilman.[7])

dislocations, and it is also absorbed in the cleavage steps formed as a result of glide in front of the crack. For the size of loops observed in LiF ($\sim$5-μ diameter), Gilman [9] estimates the first of these terms to be about 10^3 ergs/cm^2 (that is, of the order of the surface energy of the material), and the second to be of the order of the surface energy for single screw dislocation steps and up to 100 times the surface energy for very large steps.

It is to be expected then that, as a crack slows down below the critical velocity and dislocations are nucleated at the tip of the crack, it will be

slowed down further and will eventually stop unless energy can be continuously supplied. In the limit then, one would not expect it to be possible to propagate a cleavage crack slowly except in exceptional cases where the cohesive strength of the cleavage plane is very low compared to the resistance to glide in the glide planes that are oblique to the cleavage plane.

In many of the crystalline materials that exhibit cleavage fracture, temperature is one of the most important variables affecting the resistance

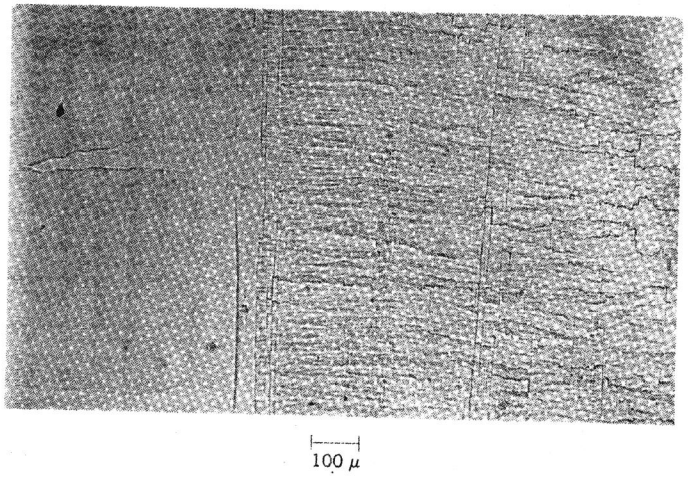

Fig. 8. Change in density of cleavage steps with change in temperature of cleavage. Zinc single crystal partially cleaved at 78°K, cleavage continued at 300°K. 78°K cleavage on left, 300°K cleavage on right.

to glide. It is to be expected, therefore, that the extent of the glide occurring at the tip of a crack will be strongly affected by the temperature of propagation. This effect is illustrated in Fig. 8 for a zinc crystal that was partially cleaved at 78°K and then cleaved further at 300°K. The difference in the number of cleavage steps at 300°K compared to 78°K is quite striking, and it has a very strong effect on the propagation. At 78°K, the crystal could be cleaved by a single light blow on a wedge aligned with the cleavage plane; at 300°K, cleavage could be achieved only by continuously forcing a wedge between the two cleaved surfaces, and even then, the crack propagated in a discontinuous fashion. From these observations, it might be expected that at some still higher temperature the amount of glide at the crack tip would become so large that cleavage would become impossible, and parting would occur by a ductile rupture process rather than by cleavage.

Cleavage Fracture of Polycrystalline Aggregates

Where the orientation change across a boundary is not too large, the crack front crosses the boundary with no change except for the appearance of large cleavage steps originating at the boundary. This effect is illustrated in Fig. 9 and in several of the other polycrystalline fractographs that follow. The tilt-twist boundary of Fig. 9 is of particular interest because of the radiating step pattern between the large cleavage steps. These steps suggest that the crack crossed this boundary by the nucleation of a series of new cracks on different levels all along the boundary.

In a randomly oriented aggregate, as judged from the direction of the river patterns within individual grains, the propagation of the crack front is extremely irregular, and the cleavage cracks may in some regions be propagating in a direction opposite to the mean direction of propagation. These effects are illustrated in Fig. 10, in which the arrows indicate the direction of crack propagation from point to point over this portion of the fracture. Also of interest in Fig. 10 are the transitions that occur at the several grain boundaries. The generation of large cleavage steps similar to those of Fig. 9 may be seen, and in addition, there are at some boundaries dark irregular bands where the carbon replicating film has collapsed, suggesting very large level differences or intergranular cracks at these boundaries. The details of how the individual grain cleavage cracks are joined along such boundaries is obscured by the collapse of the replicating film, but they are probably regions of considerable distortion such as the one shown at the junction of two cleavage cracks in Fig. 11.

As Crussard [11] has reported from his observations on the fracture surfaces of Charpy impact bars, there is also evidence for discontinuous crack propagation in these polycrystalline aggregates. Such evidence is illustrated in Fig. 12, where all of the river patterns radiate from a point in the center of the photograph, indicating that a new crack has been nucleated in front of the main crack. The importance of this observation lies in the fact that such discontinuously nucleated cracks will probably be on different levels from the main crack and will cause the formation of "tearlines" where the two cracks join, such as those observed by Kies, Sullivan, and Irwin [12] for a variety of materials.

Finally, as illustrated in Fig. 13, some grains may be so poorly oriented for cleavage that they fail by heavy plastic deformation and ductile rupture. This is not a common observation; however, Crussard [11] has observed that even in impact tests at 78°K the fracture surface of a polycrystalline specimen will contain some areas of ductile rupture.

All of the above observations lead to the qualitative conclusion that

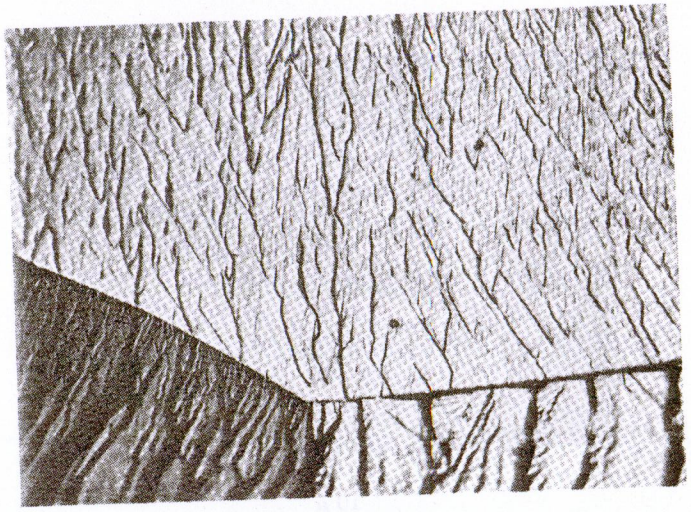

Fig. 9. Cleavage steps originating at two high-angle boundaries. Left boundary approximately 10° tilt; right boundary approximately 10° tilt plus 3° twist. Note radiating pattern between large cleavage steps right boundary. 3% Si-Fe cleaved at 78°K, direction of crack propagation top to bottom.

Fig. 10. Cleavage pattern of polycrystalline iron at 78°K. Approximately 0.02-mm grain size; broken in tension; reduction in area to fracture 26.5%. Note variability of direction of propagation of crack from grain to grain and dark irregular bands at some grain boundaries (see Fig. 11). Electron micrograph.

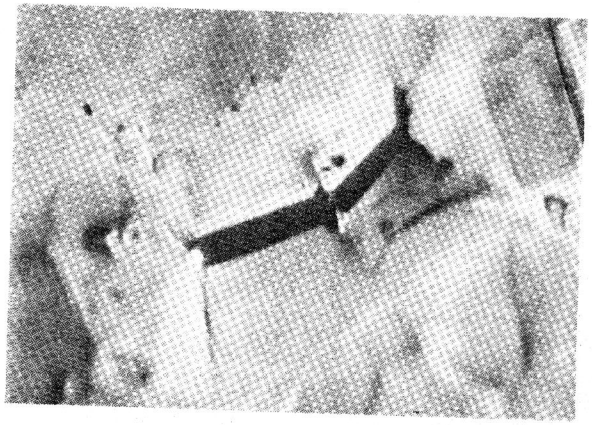

10 μ

Fig. 11. Example of distorted region at grain boundary between cleaved grains in polycrystalline iron deformed 7.5% in bending at 78°K.

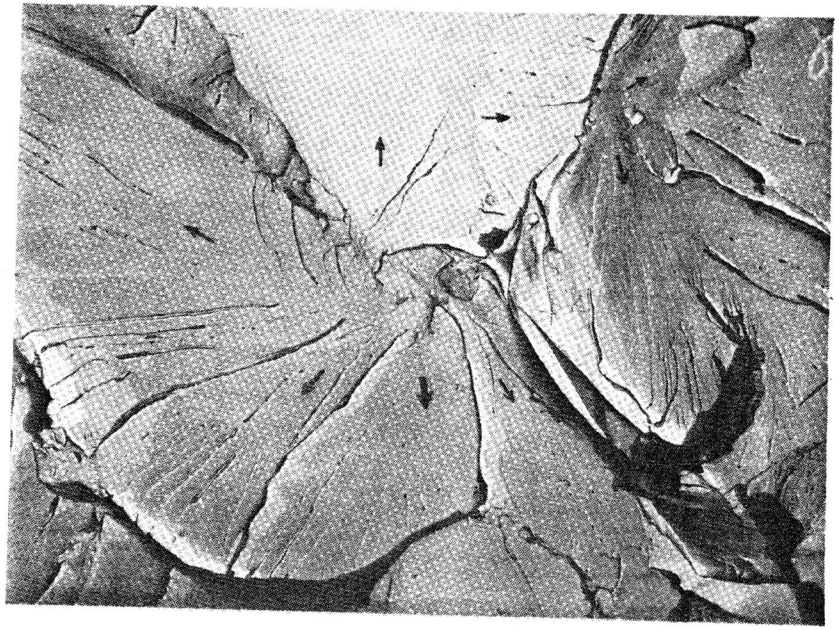

1 μ

Fig. 12. Example of cleavage step pattern radiating from a point in polycrystalline iron fractured at 78°K. Arrows indicate direction of crack propagation as deduced from river patterns. Electron micrograph.

cleavage fracture should be much more difficult to propagate in a polycrystalline aggregate than in a single crystal. Furthermore, since most of the energy-absorbing processes are associated with the boundaries between differently oriented grains, one would expect that, the finer the grain size, the more difficult would be the process of crack propagation. There do not appear to be any quantitative measurements of the specific energy required for brittle crack propagation in fine- and coarse-grained materials; however, the observations mentioned here suggest that the generally observed improvement in resistance to brittle fracture which may be achieved in a given material by a decrease in grain size results from an improved resistance to crack propagation, as well as from an improved resistance to crack nucleation.

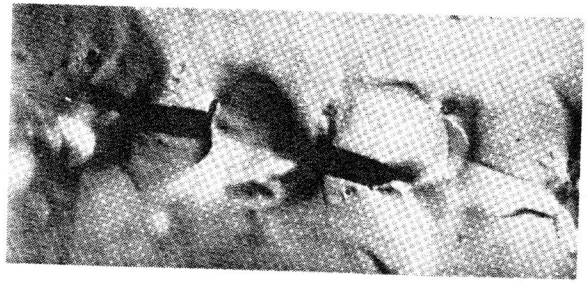

10 μ

Fig. 13. Example of heavily deformed grain between two cleaved grains. Polycrystalline iron deformed 7.5% in bending at 78°K.

Cleavage Fracture of Two-Phase Aggregates

It is now well established that the resistance to brittle fracture of a single steel may vary over wide limits depending upon the microstructure.[13] In addition to the grain-size effect, which is analogous to that observed in single-phase aggregates, a steel transformed to martensite or lower bainite is found to be greatly superior to the same steel if transformed to pearlite or upper bainite. A recent study of the brittle fracture surfaces of these various austenite decomposition products by Turkalo [14] contributes greatly to the understanding of why the acicular low-temperature transformation products are so superior to the higher-temperature transformation products. In this study, specimens of a 0.56% carbon steel were austenitized to give a No. 7 ASTM grain size. They were then transformed to pearlite, upper bainite, lower bainite, or martensite, all tempered to the same hardness level, and then fractured at 78°K. The fracture surfaces were then examined by electron microscopy.

Figure 14 is a typical example of a section through a cleavage fracture of pearlite. Most of the fracture surface is made up of cleavage facets traversing *several* pearlite colonies, with occasional regions where the fracture path follows an intercolony boundary. An example of inter-

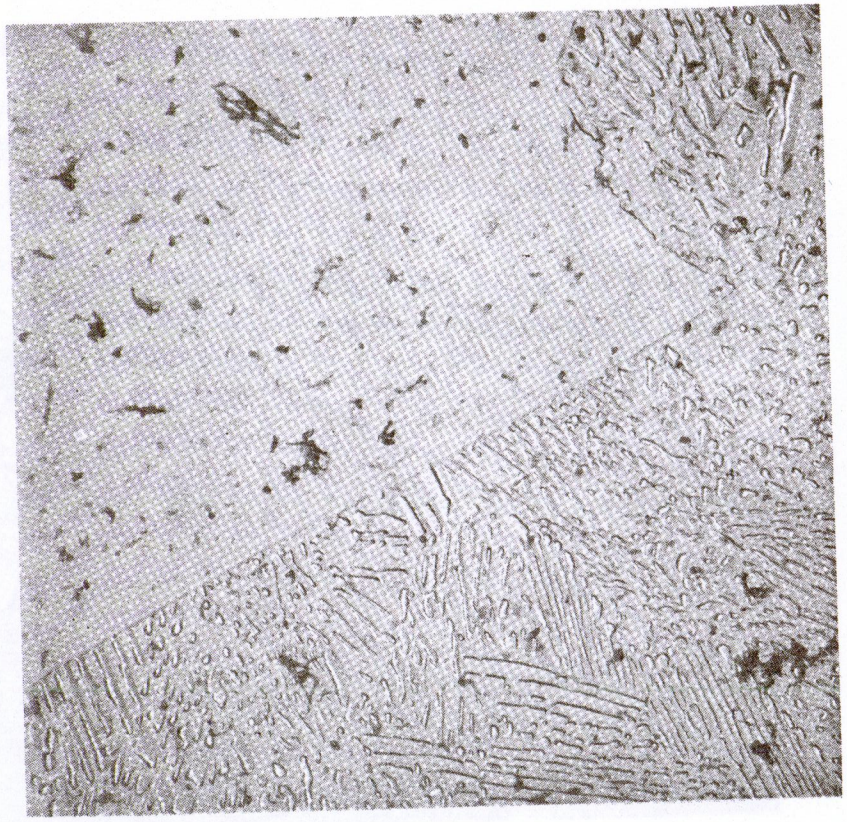

Fig. 14. Example of single cleavage facet extending over several pearlite colonies. 0.56% carbon pearlitic steel broken by notched-bar impact at 78°K. Nickel-plated fracture surface. Electron micrograph.

colony fracture is shown in Fig. 15. The important observations here are that the single cleavage facet may cut across several pearlite colonies. In some cases it was observed that a single cleavage facet traversed the whole of an austenite grain, even though the austenite grain was made up of a number of pearlite colonies. Since the fracture path is controlled by the ferrite, this implies that the ferrite from a single austenite grain

may have preferred orientation such that the cleavage planes in adjacent pearlite colonies are closely aligned.

Figure 16 is an example of the fracture appearance of the upper-bainite structure. Here again, as in the case of pearlite, the fracture path appears

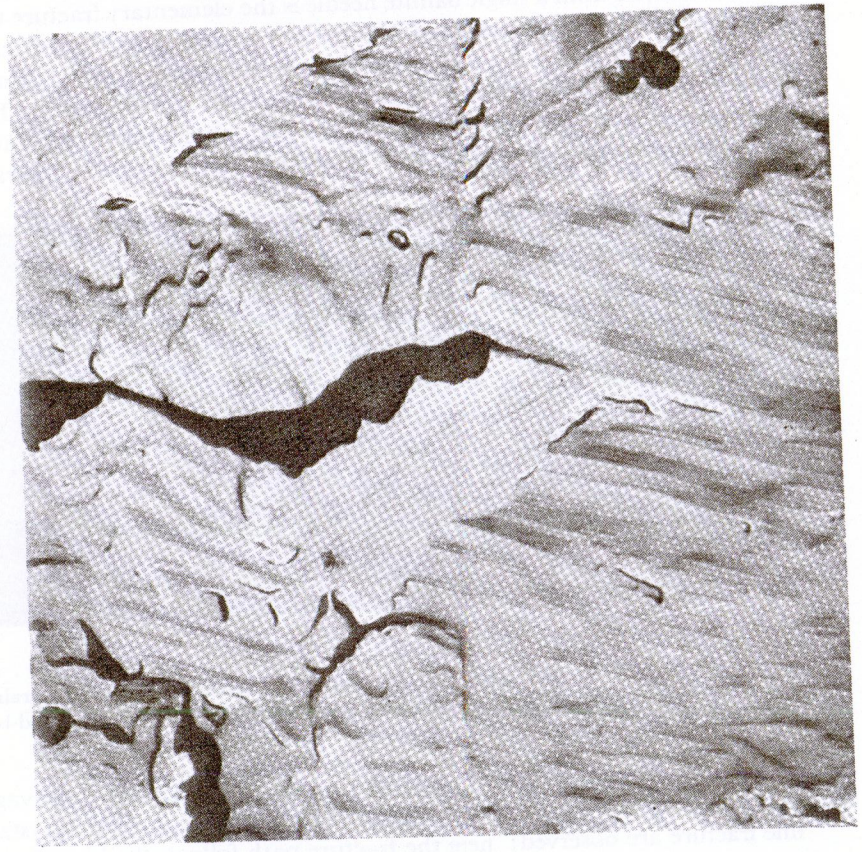

Fig. 15. Example of intercolony fracture surface on pearlite. Electron micrograph.

to be controlled by the ferrite phase with some perturbation by the distributed carbides. Also, as in the case of pearlite, the fracture facet traverses *several* bainite grains, implying alignment of the ferrite within a single austenite grain. This latter conclusion is supported by Yukawa's observation [15] that the size of secondary cleavage cracks in fractured bainitic steels increases with increasing austenitizing temperature.

In contrast to the above observations on pearlite and upper bainite, the fracture surface of tempered *lower* bainite is made up of many fine cleavage facets. As Figs. 17 and 18 show, the facet size is related, not to the austenite grain size, but to the lower-bainite needle size. This suggests that the ferrite from a single bainite needle is the elementary fracture unit, and the needle boundaries may be expected to act as barriers to crack propagation in much the same way as grain boundaries do in a single-phase aggregate. This also means, of course, that the elementary fracture unit in this case is much smaller than that for the high-temperature transformation products where the size of this unit may be comparable

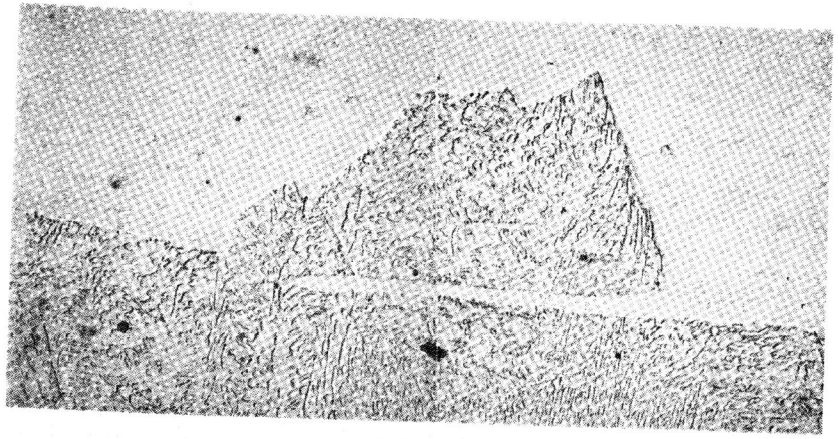

Fig. 16. Example of single cleavage facet extending over several upper-bainite grains. Bainite formed by reaction at 400°C and tempered at 565°C; broken by notched-bar impact at 78°K. Nickel-plated fracture surface. Electron micrograph.

to the austenite grain size. In addition to the transcrystalline cleavage that makes up the bulk of the fracture surface, some areas of intercrystalline fracture are observed; here the fracture path follows the boundaries between the very small ferrite grains that are formed when lower bainite is tempered.

The observations on tempered martensite fracture surfaces, Fig. 19, are similar to those on tempered lower bainite. Again the cleavage facets are governed primarily by the martensite needle size, and again some ferrite intercrystalline fracture is observed.

One other observation on the fracture appearance for *untempered* martensite is of interest. In the quenched condition, approximately 50% of the fracture surface is intercrystalline fracture following the former austenite grain boundaries, Fig. 20. Thus, tempering not only modifies

the martensite needle structure but also eliminates the austenite grain-boundary weakness of the as-quenched martensite.

It appears, then, that the brittle fracture of all of these austenite decomposition products is governed primarily by the ferrite. In the high-

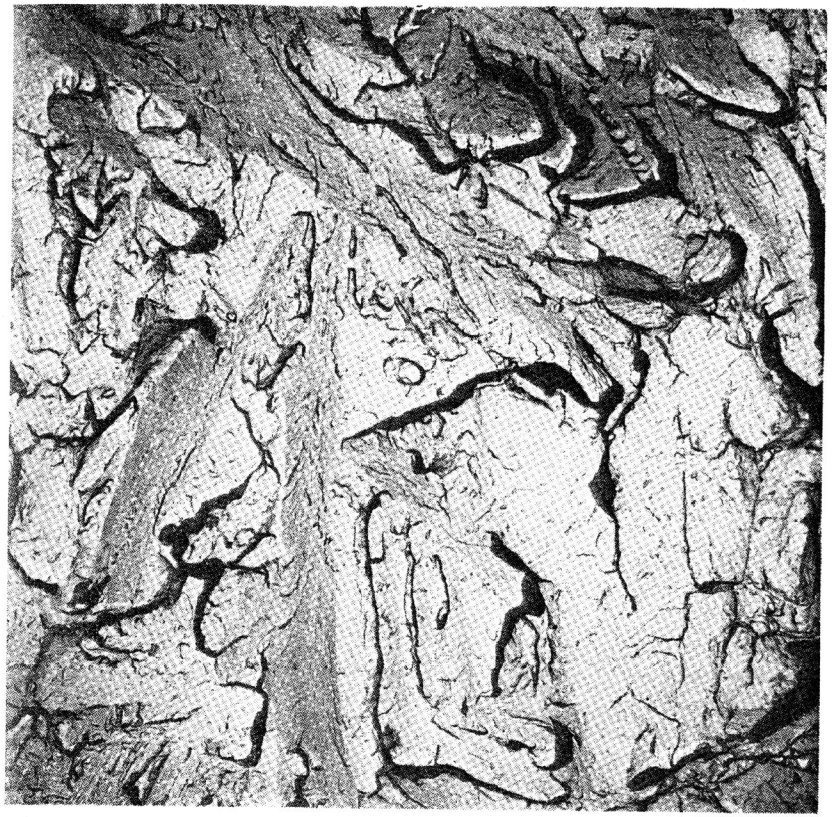

Fig. 17. Fractograph of untempered lower bainite formed by reaction at 300°C and broken by notched-bar impact at 78°K. Note acicular character of many of the cleavage facets. Electron micrograph.

temperature products, pearlite and upper bainite, cleavage may proceed over long distances without interruption, with a single cleavage facet often traversing several pearlite colonies or bainite grains. For these structures, one would expect to improve the resistance to brittle fracture only by refining the austenite grain size. On the other hand, for the acicular products (lower bainite and martensite), the needle size appears

to control the fracture, and an improvement here would be achieved by reducing the needle size.

Fig. 18. Fractograph of lower bainite of Fig. 17 after tempering at 560°C. Acicular cleavage facets still present but not as clearly marked as in Fig. 17. Electron micrograph.

Intergranular Brittle Fracture

In attempting to improve the resistance to brittle fracture of any polycrystalline material, it is important to determine whether the brittle fracture occurs by transcrystalline cleavage or by separation along grain boundaries. If the brittle fracture is intergranular, then none of the conclusions concerning the effect of microstructure on cleavage fracture will apply. Intergranular brittle fractures fall into two classes: those

in which a film of a brittle phase separates at the grain boundaries and those in which the grain boundary is embrittled, presumably by im-

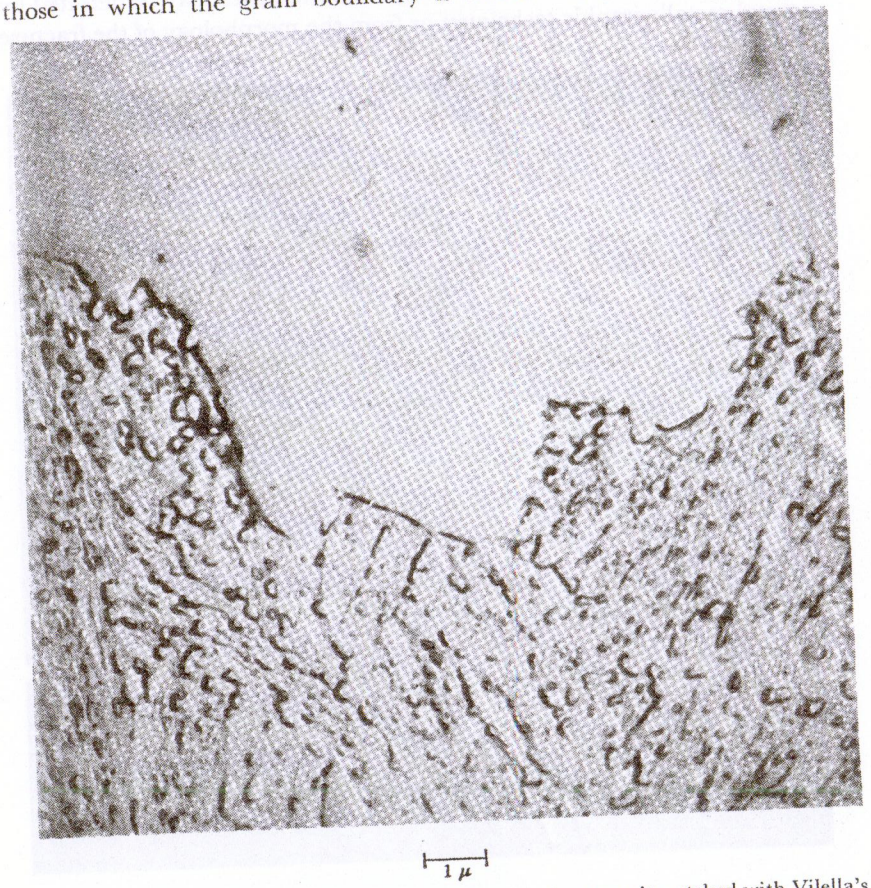

Fig. 19. Section of nickel-plated fracture of tempered martensite, etched with Vilella's reagent. Note change in direction of fracture at boundaries of martensite needles. Electron micrograph.

purity segregation alone, without the appearance of a separated phase.

Plateau, Henry, and Crussard [16,17] have described a number of cases of intergranular fracture resulting from the formation of filmlike precipitates at grain boundaries. Notable among these were several austenitic chromium-nickel steels which had been embrittled by intergranular carbide precipitation. These investigators found that the grain-boundary films need not be continuous to produce intergranular fracture. Usually the precipitates took the form of flat dendrites covering perhaps 50% of the grain surface, with fracture occurring sometimes at the carbide-

matrix interface and sometimes by cleavage of the thin carbide plates. Such thin, discontinuous films at the grain boundaries may be detected by normal metallographic techniques or from the morphology of the fracture

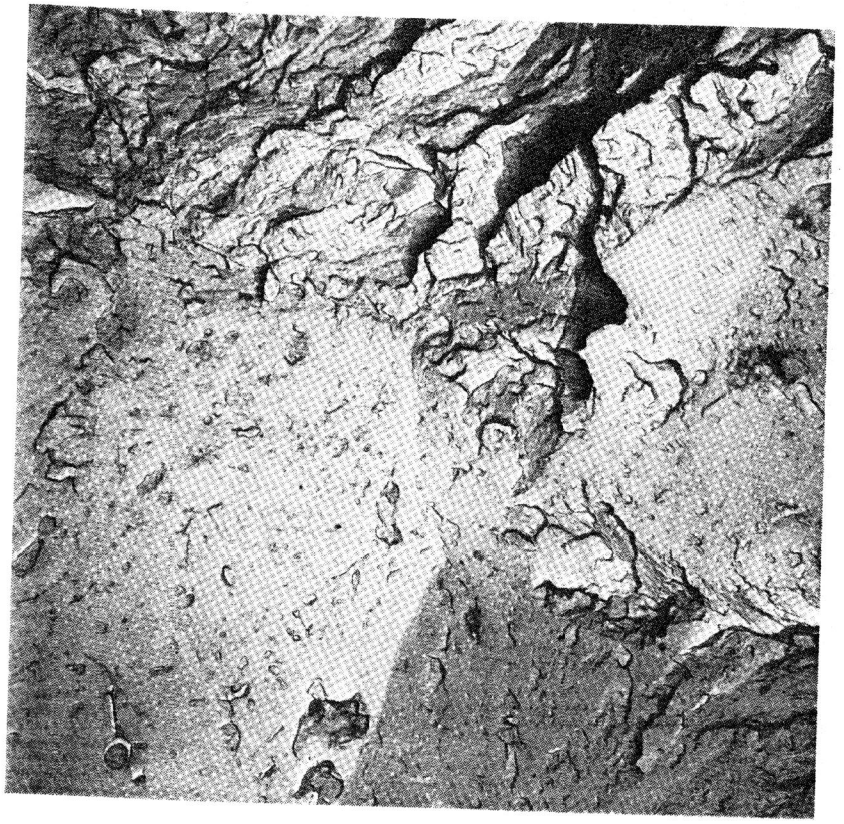

Fig. 20. Fractograph of untempered martensite broken at 78°K. Upper one third transcrystalline, lower two thirds intercrystalline fracture at austenite grain boundaries. Electron micrograph.

surface, but they are best revealed by etching the fracture surface. Wulff [18] has also shown that the embrittlement of molybdenum by trace amounts of oxygen, nitrogen, or carbon is due to the formation of thin second-phase films often not detectable in a normal metallographic section but clearly revealed by metallographic examination of fracture surfaces.

There remain a number of cases of brittle, intergranular fracture for which it has not been possible to detect second-phase films at the grain

boundaries. These are the embrittlement of copper by antimony,[19] temper brittleness in alloy steels,[17,20,21] and the embrittlement of iron by oxygen.[17,22,23]

Figure 21 is a photomicrograph of the intergranular fracture surface of an iron specimen containing about 0.02% oxygen that was decarburized and then fractured at 78°K. In contrast to the cleavage step pattern

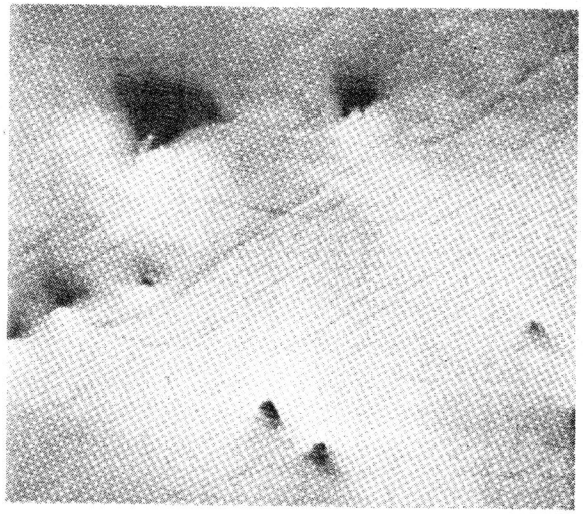

Fig. 21. Fractograph of 0.02% oxygen, decarburized iron broken at 78°K. Intergranular fracture. Note extreme smoothness of fracture surface and general absence of cleavage steps.

usually observed in transcrystalline fracture (Figs. 1, 11, 12), this fracture is extremely smooth and follows the grain surface precisely. The only structural features of this fracture surface are the small nonmetallic inclusions distributed on the grain surface. These are, however, so widely dispersed that they can hardly be considered to have caused the embrittlement.

Figure 22 shows electron microscope pictures of the intergranular fracture surfaces of a 0.40% carbon, 3.50% Ni, 1.5% Cr steel in the non-embrittled and in the temper-embrittled condition. By coarsening the austenite grain size of this steel, it was possible to obtain an intergranular fracture even in the unembrittled condition. This then made possible the comparison of grain-boundary fracture surfaces before and after embrittlement. Despite the fact that the embrittlement treatment shifted the

Charpy transition temperature upward by about 200°C, it has not been possible to detect any difference in these two fracture surfaces. The surfaces were examined as-fractured, after etching with various reagents, and by extraction replication. All that is revealed by these various methods is the structure of the tempered martensite making up the grains themselves, with no indication of any structural features associated with the boundary or the propagation of a crack along the boundary.

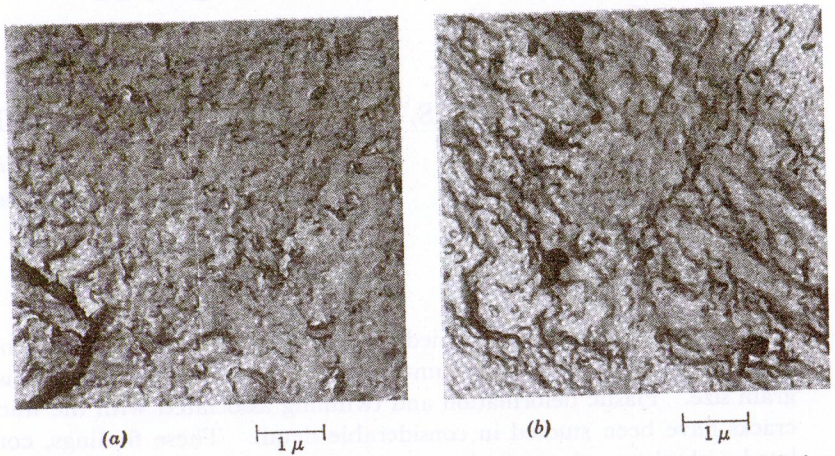

Fig. 22. Fractographs of intergranular fracture surface of AISI 3340 steel before (*a*) and after (*b*) temper embrittlement. Embrittled 16 hr at 500°C. Electron micrographs.

Observations such as those just cited for temper embrittlement and the iron-oxygen alloy have led McLean and Northcott,[24] McLean,[19] and Woodfine [25] to propose that embrittlement may occur by an equilibrium segregation of impurities at the boundary without the formation of a second phase between the matrix grains. At the present time, except for certain grain-boundary etching effects which appear to correlate with embrittlement,[26] this segregation remains to be demonstrated, and a more detailed mechanism for embrittlement by segregation is required.

Summary

The various microstructural features that influence cleavage fracture in crystalline materials have been reviewed.

In the case of single crystals, screw dislocations have the greatest impeding effect on the propagation of cleavage cracks, since they cause cleavage steps. Such dislocations may be present as grown-in dislocation networks or as arrays of dislocations in subboundaries, or they may be introduced by plastic deformation. This plastic deformation may occur at the tip of the advancing crack if the rate of crack propagation is low enough or if the temperature is high enough.

In the case of a randomly oriented polycrystalline aggregate, the change in orientation at individual grain boundaries impedes the propagation of the cleavage crack by creating cleavage steps or by causing localized deformation and tearing near the grain boundary, or in some cases whole grains may fail by ductile rather than brittle fracture.

In the one case of a two-phase aggregate examined, namely, a steel having various structures, the greater brittleness of the high-temperature reaction products, pearlite and upper bainite, is explained by the observation that the individual cleavage facets are much larger than those of the low-temperature reaction products, lower bainite and martensite. Thus, for any polycrystalline aggregate, the smaller the distance a crack may propagate without being deviated by a change in orientation of the cleavage plane, the greater will be the resistance to brittle fracture.

Intercrystalline brittle fractures constitute a special class because (1) the energy absorbed in crack propagation appears to be very low compared to transcrystalline fracture, as judged from the fracture appearance, and (2) such fractures cannot be expected to be influenced by the structural changes within the grains which might improve the resistance to transcrystalline brittle fracture.

ACKNOWLEDGMENT

I am greatly indebted to Miss Ann M. Turkalo for permission to describe the results of her investigation of the effects of microstructure on the brittle fracture of steel.

REFERENCES

1. S. Tolansky, *Multiple Beam Interferometry*, Clarendon Press, Oxford (1949).
2. J. J. Gilman, *J. Appl. Phys.*, **27**, 1262 (1956).
3. J. M. Berry, "Cleavage Step Formation in Brittle Fracture Propagation," Amer. Soc. Metals preprint (1958).
4. J. R. Low, Jr., I.U.T.A.M. Colloquium, Madrid, *Deformation and Flow of Solids*, R. Grammel, Ed., Springer-Verlag, Berlin, p. 60 (1956).
5. D. K. Roberts and A. A. Wells, *Engineering*, **178**, 820 (1957).
6. J. J. Gilman, *Trans. AIME*, **203**, 1252 (1955).
7. J. J. Gilman, *Trans. AIME*, **212**, 310 (1958).
8. J. J. Gilman, C. Knudsen, and W. P. Walsh, *J. Appl. Phys.*, **29**, 601 (1958).
9. J. J. Gilman, *Trans. AIME*, **209**, 449 (1957).

10. W. G. Johnston and J. J. Gilman, *J. Appl. Phys.*, **30,** 129 (1959).
11. C. Crussard, R. Borione, J. Plateau, Y. Morillon, and F. Maratray, *J. Iron Steel Inst. (London)*, **183,** 146 (1956).
12. J. A. Kies, A. M. Sullivan, and G. R. Irwin, *J. Appl. Phys.*, **21,** 716 (1950).
13. J. H. Hollomon, L. D. Jaffe, D. E. McCarthy, and M. R. Norton, *Trans. Amer. Soc. Metals*, **38,** 807 (1947).
14. A. M. Turkalo, "The Morphology of Brittle Fracture of Pearlite, Bainite and Martensite," to be published.
15. S. Yukawa, "Relation of Cleavage Crack Size to Austenitizing Conditions for Ni-Mo-V Steels," unpublished research.
16. J. Plateau, G. Henry, and C. Crussard, *Rev. mét.*, **54,** 3 (1957).
17. J. Plateau, G. Henry, and C. Crussard, *Rev. universelle mines*, **12,** 1 (1956).
18. H. S. Spacil and J. Wulff, *The Metal Molybdenum*, Amer. Soc. Metals, Cleveland, p. 262 (1958).
19. D. McLean, *J. Inst. Metals*, **81,** 121 (1952).
20. J. Nutting and V. E. Cosslett, *Metallurgical Applications of the Electron Microscope*, Institute of Metals, London (1950).
21. B. C. Woodfine, *J. Iron Steel Inst. (London)*, **173,** 229 (1953).
22. W. P. Rees and B. E. Hopkins, *J. Iron Steel Inst. (London)*, **172,** 403 (1952).
23. J. R. Low, Jr., and R. G. Feustel, *Acta Met.*, **1,** 185 (1953).
24. D. McLean and L. Northcott, *J. Iron Steel Inst. (London)*, **158,** 169 (1953).
25. B. C. Woodfine, *J. Iron Steel Inst. (London)*, **173,** 240 (1953).
26. J. B. Cohen, A. Hurlich, and M. Jacobson, *Trans. Amer. Soc. Metals*, **39,** 109 (1947).